Published in final edited form as:
Cell Host Microbe. 2013 December 11; 14(6): . doi:10.1016/j.chom.2013.11.004.

Natural Killer Cell-Mediated Host Defense against Uropathogenic *E. coli* Is Counteracted by Bacterial HemolysinA-Dependent Killing of NK Cells

Chamutal Gur[1,4,6], **Shunit Coppenhagen-Glazer**[2,6], **Shilo Rosenberg**[3], **Rachel Yamin**[1], **Jonatan Enk**[1], **Ariella Glasner**[1], **Yotam Bar-On**[1], **Omer Fleissig**[1,2], **Ronit Naor**[2], **Jawad Abed**[2], **Dror Mevorach**[4], **Zvi Granot**[5], **Gilad Bachrach**[2,6,*], and **Ofer Mandelboim**[1,6,*]

[1]The Lautenberg Center of General and Tumor Immunology, The Hebrew University Hadassah Medical School, IMRIC, Jerusalem 91120, Israel

[2]The Institute of Dental Sciences, Hebrew University-Hadassah School of Dental Medicine, Jerusalem 91120, Israel

[3]Urology Department Hadassah Medical Center, Jerusalem 91120, Israel

[4]Internal Medicine Department Hadassah Medical Center, Jerusalem 91120, Israel

[5]Department of Developmental Biology and Cancer Research, The Hebrew University Hadassah Medical School, IMRIC, Jerusalem 91120, Israel

SUMMARY

Uropathogenic *Escherichia coli* (UPEC) are a common cause of urinary tract infections (UTIs) in humans. While the importance of natural killer (NK) cells in innate immune protection against tumors and viral infections is well documented, their role in defense against bacterial infections is still emerging, and their involvement in UPEC-mediated UTI is practically unknown. Using a systematic mutagenesis approach, we found that UPEC adheres to NK cells primarily via its type I fimbriae and employs its hemolysinA toxin to kill NK cells. In the absence of hemolysinA, NK cells directly respond to the bacteria and secrete the cytokine TNF-α, which results in decreased bacterial numbers in vitro and reduction of bacterial burden in the infected bladders. Thus, NK cells control UPEC via TNF-α production, which UPEC counteracts by hemolysinA-mediated killing of NK cells, representing a previously unrecognized host defense and microbial counterattack mechanism in the context of UTI.

INTRODUCTION

E. coli colonize the gastrointestinal tract of human infants within a few hours after birth (Kaper et al., 2004). This commensal bacterium rarely causes disease except in immunocompromised hosts (Kaper et al., 2004). However, there are several highly adapted pathogenic *E. coli* strains that cause a broad spectrum of diseases, including enteric disease, sepsis/meningitis, and UTI (Emody et al., 2003; Johnson, 1991). UPEC is responsible for approximately 80%–90% of community-acquired UTI cases (Sivick et al., 2010; Ulett et al., 2013), and around 50% of all women and 12% of men will experience at least one episode

*Correspondence: giladba@ekmd.huji.ac.il (G.B.), oferm@ekmd.huji.ac.il (O.M.) http://dx.doi.org/10.1016/j.chom.2013.11.004.

[6]The first two authors and the last two authors contributed equally to this work

SUPPLEMENTAL INFORMATION Supplemental Information includes five figures and one table and can be found with this article at http://dx.doi.org/10.1016/j.chom.2013.11.004.

Europe PMC Funders Author Manuscripts

of a clinically significant infection during their lifetime (Sivick et al., 2010). UPEC utilize virulence factors that are encoded on pathogenicity islands (Ulett et al., 2013) to infect an immunocompetent host by colonizing the periurethral area and subsequently ascend through the urethra to the bladder (Kucheria et al., 2005). In the bladder, uroepithelial cells are the early sensors of microbial challenge (Ragnarsdóttir et al., 2011). Neutrophils are the first and most-abundant cell type to migrate to the bladder in the event of UTI, and they constitute a crucial limiting factor for bacterial growth in the urinary tract (Haraoka et al., 1999). In addition, other immune cells have also been implicated in host defense against UTI (Engel et al., 2006; Jones-Carson et al., 1999). However, it is practically unknown whether NK cells, which are critical players in the innate immune response, are present in the bladder or involved in UTIs.

NK cells are lymphocytes which make up to 15% of all peripheral blood lymphocytes (Seidel et al., 2012). They are best known for their ability to kill virally infected and transformed cells and for secreting cytokines, specifically TNF-α and IFN-γ (Jewett et al., 1996). The NK cell activity is regulated through a balance of signals derived from inhibitory and activating receptors (Koch et al., 2013). Their ligands are numerous and can be stress induced, tumor derived, pathogen derived, and even self-ligands (Seidel et al., 2012). While the importance of NK cells in innate immune protection against tumors or viral infections is well documented (Koch et al., 2013), their ability to directly recognize bacteria is less well defined. In this regard, we have previously shown that NK cells are able to directly recognize *Fusobacterium nucleatum* through their killer receptor NKp46 and that this interaction exacerbated periodontal disease (Chaushu et al., 2012).

In this study we show in vitro that strains of UPEC adhere to human and murine NK cells primarily through their type I fimbria and kill NK cells via their hemolysinA toxin. We demonstrate in vivo that NK cells accumulate in the bladder during UTI and that in the absence of hemolysinA the interaction between NK cells and *E. coli* leads to TNF-α secretion, which attenuates the infection. In contrast, pathogenic UPEC strains that express hemolysinA evade this NK cell control by killing the NK cells.

RESULTS

Strains of UPEC Kill Human NK Cells

To test whether bacteria are directly recognized by NK cells, we incubated several bacterial strains (Figure S1 available online), including GFP-expressing *E. coli* strains (Figure 1) with human NK cells. The incubation was performed either at 4°C or at 37°C. NK cells were analyzed by flow cytometry for GFP (indicative of bacterial binding) and for PI (to detect dead cells). As can be seen in Figure 1A, at 4°C (upper dot plots) we observed enteric (EPEC) and urinary pathogenic *E. coli* strains: UPEC SR71 and UPEC CFT073 (cystitis and pyelonephritis isolates, respectively) adhered to about 20% of the NK cells. When the bacteria were incubated with the human NK cells at 37°C, they interacted with higher percentages of NK cells (lower dot plots, Figure 1A), and to our surprise a substantial (around 72%, upper quadrants) PI staining (indicative of cell death) was observed with UPEC CFT073 (Figure 1A). This pattern of PI staining was not seen with XL1 or with the UPEC SR71 strain, nor was it observed with EPEC or with other bacterial species tested (Figure S1).

The PI staining observed with the UPEC CFT073 bacterium was accompanied by changes in the morphology of the NK cells. As can be seen in Figure 1B, at 37°C, in the presence of UPEC CFT073 the NK cells appeared smaller and were mostly present in gate 2 (the cells in this gate were stained positive for PI). In contrast, when NK cells were incubated with UPEC CFT073 at 4°C, a normal NK cell morphology was evident, and most cells were

present in gate 1 (the NK cells in this gate are mainly PI negative). Furthermore, at 4°C, the NK cell population in gate 1 was more or less equivalent in size to the population of NK cells observed when UPEC CFT073 is absent (Figure 1B). Figures 1C and 1D summarize and quantify these observations. As can be seen, little or no changes were observed when bacteria other than UPEC CFT073 were used. To further corroborate our findings, we used confocal microscopy, and as can be seen in Figure 1E, nearly all NK cells were stained positive for PI when incubated at 37°C for 3 hr with UPEC CFT073. The bacteria, on the other hand, remained PI negative when incubated with the NK cells either at 37°C (Figure 1E) or at 4°C (data not shown), suggesting that the bacteria are not killed by the NK cells. To determine whether UPEC CFT073 invades the NK cells, we incubated the NK cells for 3 hr at 37°C with the GFP-labeled UPEC CFT073 bacterium and stained the human NK cells with the anti-CD56 mAbs that primarily stain the NK cell membrane (Figure 1F, left). As can be seen, the UPEC CFT073 bacterium does not seemed to penetrate into the dead human NK cells. Scanning electron microscopy (SEM), (Figure 1F, right) and transmission electron microscopy (TEM) (Figure 1F, bottom) experiments indeed demonstrated that the bacteria are not found inside the NK cells.

To investigate whether (1) NK cell killing is a phenomenon unique to the UPEC CFT073 strain only or (2) NK cell killing relates to the type of pathology caused by different isolates (cystitis versus pyelonephritis), we incubated additional strains of urinary pathogenic *E. coli* (UTI536, ATCC 25922, and UTI89) with human NK cells. The various *E. coli* strains were incubated at various time points (Figure 1G) and at varying ratios of bacteria to NK cells (Figure 1H). As can be seen in Figure 1G, even following 4 hr of incubation with SR71 and XL1 NK cell death was not detected. At longer time points the bacteria grow to such an extent that their overabundance caused nonspecific NK and bacteria death. Following 4 hr of incubation of CFT073, UTI536, UTI89, and ATCC 25922 with the NK cells, nearly 100% NK cell death was observed (Figure 1G). The UTI536 bacterium was exceptionally efficient at killing human NK cells, as around 60% of the NK cells were killed following 2 hr incubation with this strain, as opposed to around 30% killing observed with the other UPEC “killer” strains (Figure 1G). When repeating the experiments for 3 hr at various bacteria to NK cells ratios, UTI536 was again extremely efficient in killing the NK cells (Figure 1H). To test whether the UPEC-mediated killing is specific to NK cells, we incubated primary T and NK cells with the GFP-labeled UPEC CFT073 at 4°C and at 37°C (Figure 2). As can be seen, while the bacterium binds both T and NK cells at equivalent levels (Figure 2A), the T cells (Figure 2B) were almost completely resistant to the UPEC CFT073-mediated killing, while the NK cells were highly sensitive (Figure 2B).

UPEC CFT073 Adheres to NK Cells via Type I Fimbriae and Kills NK Cells via HemolysinA

To identify the component(s) by which UPEC adheres and kill the NK cells, we generated transposon-based insertion-inactivation mutant library in GFP-expressing UPEC CFT073 bacterium. To identify the genes involved in UPEC CFT073 adhesion, we incubated the mutant bacteria at 4°C, and to identify the killing/lytic components, we incubated the mutants for 3 hr with NK cells at 37°C. More than 1,000 clones were screened. Nine UPEC CFT073 mutants were found to be impaired in their adhesion (Figure 3A), but not in NK cell killing (Figure 3B), and three mutants were identified, having an intact adhesion ability (Figure 3C) but impaired killing activity (Figure 3D). One irrelevant mutant, B5, is shown in Figure 3 and throughout the paper. In eight of the nine UPEC CFT073 adhesion mutants, the transposon was inserted in the operon encoding for the type I fimbriae, or in type I fimbriae-associated genes (Figure 3E). The gene disrupted in the ninth mutant was tRNA uridine (Figure 3E). Interestingly, none of these mutants completely lost their adhesion potential, and as can be seen, even ~50% reduction in adhesion was still sufficient to kill NK cells after 3 hr of incubation at 37°C (Figures 3A and 3B). The disrupted genes of the three

killing mutants were also identified (Figure 3E) and were found to reside on the *hly*A operon that encodes for the hemolysinA toxin. Two mutants were found to be defective both in adhesion to NK cells and in killing the NK cells (Figures S2A and S2B, respectively). Sequencing of the disrupted genes revealed that both are housekeeping genes (Figure S2C), which are essential for bacterial growth (Figure S2D). The growth and the biological properties of all other relevant mutants were normal (Figure S2D).

Increased Adhesion through the Type I Fimbriae Leads to Increased Killing of NK Cells

The expression of the fimbriae is regulated by an invertible element which alternates between an “on” and an “off” orientation (Kaper et al., 2004; Ulett et al., 2013; Hannan et al., 2008). To further validate our findings, two additional GFP-expressing mutants of UPEC CFT073 bacteria were tested: one in which the fimbriae has been locked in an “ON” orientation (Fim on) and another that was locked in an “OFF” orientation (Fim off). In addition, we tested whether P-fimbria (Mobley et al., 1993) might be involved in the residual adhesion to NK cells by using a GFP-expressing P-fimbriae mutant (PAP–, also known as UPEC76). As can be seen (Figure 4A), when the Fim off bacterium was used, the adhesion was reduced by around 50%, and the absence of the P-fimbriae had no effect. The binding of the Fim on mutant was much stronger than all other bacteria, and around 85% of the NK cells were bound by the bacterium.

The increased adhesion observed with the Fim on also led to increased killing of NK cells. As can be seen in Figure 4B, at a ratio of 30:1, at 1 hr following incubation of the Fim on bacterium with the NK cells around 30% killing was observed, whereas practically no killing was detected with all other bacteria. Following 4 hr of incubation, around 100% killing of NK cells was detected with all bacteria, except with the Fim off bacterium, in which killing of the NK cells did not exceed 70%. Regarding varying the bacteria:NK cell ratios, already at the 7.5:1 ratio the killing of NK cells by the Fim on bacterium was very efficient compared to other bacteria tested (Figure 4C). At the 30:1 ratio, between 80%–90% of the NK cells were killed, depending on the bacteria used; however, as above (Figure 4B), the killing of NK cells by the Fim off bacterium did not exceed 70% (Figure 4C).

The Extent of HemolysinA Activity Determines the Efficiency of NK Cell Killing

HemolysinA is a cytolytic pore-forming toxin which contributes to tissue injury and erythrocyte hemolysis (Cavalieri et al., 1984; Gadeberg et al., 1983). We therefore next investigated whether all bacteria that killed the NK cells are able to cause erythrocyte hemolysis. As can be seen in Figure 5A, a clear zone in a blood agar plate was evident with all “NK killer” bacteria (Figure 1). In contrast, SR71 and XL1 did not perform hemolysis (Figure 5A and data not shown, respectively) and indeed lacks the *hlyA* gene (Totsika et al., 2009).

Type 1 fimbriae operon resides on a pathogenicity island along with hemolysinA and is a frequent spot for insertional mutations (Hannan et al., 2008). To confirm that the increased killing seen with the Fim on mutant (Figures 4B and 4C) resulted from the better adhesion properties of the mutant and to test whether the higher killing seen in UTI536 (Figures 1G and 1H) might be because this strain expresses two copies of the hemolysinA operon (Wiles et al., 2008), quantified hemolysis on sheep red blood cells (RBCs) was performed. As can be seen in Figure 5B, the hemolysis levels of all bacteria tested were equivalent, and the hemolysis induced by UTI536 was significantly higher.

To directly demonstrate that hemolysinA is responsible for the human NK cell killing, we restored the hemolysis phenotype in the hemolysinA mutant bacteria by transforming them with a plasmid harboring the entire UPEC CFT073 hemolysinA operon (the complemented

bacteria were designated C93C, D57C, and E49C). As can be seen in Figure 5C, hemolysis was restored in the complemented bacteria, and they also regained their ability to kill the NK cells, as determined by flow cytometry (Figures 5D and S3) and by confocal microscopy (Figure 5E).

NK Cells Accumulate in the Infected Bladder following UPEC CFT073 Infection

To investigate the physiological relevance of our findings, we initially isolated murine NK cells and incubated them with the various UPEC strains and with the three hemolysinA mutants. As can be seen, the murine NK cells were efficiently killed by “killer” bacteria, while no killing was observed either with the hemolysinA mutants (C93, D57, and E49) or with XL1 and SR71 bacteria (Figure 6A). Interestingly, mouse T cells, as opposed to human T cells (Figure 2), were also quite efficiently killed by all “killer” bacteria (data not shown).

We next tested whether murine NK cells are present in the bladder prior and following UPEC CFT073 infection. For this, we used the *Ncr1*$^{gfp/+}$ mice that we generated, in which NK cells are labeled with GFP and can easily be detected (Gazit et al., 2006). UPEC CFT073 or the hemolysinA mutant C93 bacteria were injected through catheters inserted into the bladders of 6-to 8-week-old C57BL/6 *Ncr1*$^{gfp/+}$ female mice, and NK cells were counted in the bladder prior and following bacterial inoculation. We used the C93 bacterium here and in most of following experiments because this mutant was disrupted in the structural *hly*A gene itself. The NK cell accumulation in the bladder was monitored for 6 consecutive days post-UTI induction, by harvesting the bladders and by counting the GFP-positive NK cells using flow cytometry. In the absence of bacterial infection, NK cells were hardly detected in the bladder; however, following bacterial inoculation, NK cells accumulated in the bladder (Figure 6B), and significantly more NK cells were observed in mice inoculated with the hemolysinA mutant bacterium C93 as compared to the wild-type bacterium (Figure 6B). The highest number of NK cells in the bladder was observed on day 2 following UTI induction (Figure 6B). At later time points, the NK cells gradually disappeared and were practically undetectable on day 5 postinfection (data not shown). Cryosections from bladders were also obtained at day 2 post-UTI induction, and NK cells in the bladder were viewed using confocal microscopy (Figure 6C). In agreement with the flow cytometry experiments (Figure 6B), very few or no NK cells were detected in the PBS-injected bladders, and the highest number of NK cells was observed following inoculation with the hemolysinA C93 mutant (Figure 6C, depicting a piece of the bladders’ uroepithelial cells). Figure S4 illustrates that following UPEC infection the NK cells are found mainly in the uroepithelial cells, especially in the mesenchymal area.

NK Cells Attenuate UTI through TNF-α

NK cells do not kill the bacteria directly, as incubation of NK cells with the wild-type UPEC CFT073 bacterium (Figure 1E) and with the hemolysinA mutants (Figure 5E) did not result in PI staining of the bacteria. Furthermore, no decrease in bacterial viability was detected following incubation of the various bacteria with NK cells (Figure S5). To investigate whether NK cells will produce cytokines upon their direct interaction with the bacteria, we incubated mouse NK cells with all wild-type bacteria used in this work and determined the TNF-α concentrations in the supernatants. NK cells incubated with bacteria lacking the hemolysinA toxin such as XL1 and SR71, secreted high levels of TNF-α (Figure 7A), while the amount of TNF-α secreted from NK cells incubated with the hemolytic UPEC strains was greatly reduced (Figure 7A). This is due to NK cell killing by all of the hemolytic UPEC strains (verified by PI staining at the end of the ELISA assays, data not shown). Similar results were obtained with the complemented hemolysinA bacteria and little secretion of TNF-α was noted (data not shown).

To identify the NK cell receptor mediating the TNF-α secretion, we initially investigated whether the two major murine NK-activating receptors, NKG2D and Ncr1, are able to directly recognize the bacteria. To this end, we used Ncr1-Ig and NKG2D-Ig fusion proteins, and as can be seen in Figure 7B, all the bacteria tested were not stained by the fusion proteins. In contrast, the murine thymoma PD1.6 cells previously shown to express ligand for Ncr1 (Halfteck et al., 2009) were recognized by both Ncr1-Ig and NKG2D-Ig, whereas the Ncr1-ligand-negative YAC-1 cells (Gazit et al., 2006) were recognized by NKG2D-Ig only (Figure 7B). It was previously shown that UPEC bacteria directly activate NK cells, leading to the secretion of TNF-α via TLR-4 (Mian et al., 2010). To test whether TLR-4 is involved in the TNF-α secretion, we incubated the irrelevant mutant B5 and the hemolysinA mutant C93 bacteria with murine NK cells. The C93 bacterium was incubated with NK cells that were pretreated or not with blocking anti-TLR-4 mAb. As can be seen, incubation of the NK cells with C93 led to substantial TNF-α secretion which was partially reduced by the anti-TLR-4 mAb (Figure 7C), suggesting that TLR-4 is involved in the TNF-α secretion following the direct interaction with the bacteria.

To investigate the importance of NK cells and TNF-α in vivo, we initially performed calibration experiments in which bacterial loads were evaluated in the bladders, kidneys, and blood over 6 days following bacterial inoculation, with or without depletion of NK cells using the anti-NK1.1 mAb. The efficiency of the anti-NK1.1 mAb in depleting NK cells was monitored using the Ncr1$^{gfp/+}$ mice that we have generated (Gazit et al., 2006). As can be seen in Figure 7D, NK cells were present in the blood and kidney, but not in the bladder, even prior to the bacteria inoculation. Upon bacterial injection, the NK cell numbers were reduced in the blood and concomitantly increased in the kidneys and in the bladders (Figure 7D). Injection of anti-NK1.1 mAb led to a near-complete reduction in the numbers of NK cells present in the blood, kidneys, and bladders (Figure 7D). Following these calibration experiments, we investigated the role played by NK cells and TNF-α in UTI. Three groups of mice were catheterized: group 1 was pretreated with anti NK1.1 antibody, 1 day prior to the inoculation of the bacteria and 1 day following the catheter inoculation; group 2 was pretreated with a soluble receptor for TNF-α (Etanercept) on the day of bacterial inoculation and on the following day; group 3 was left untreated (Figure 7E). The three groups of mice were further divided into four subgroups: one group received PBS, the second group received the wild-type UPEC CFT073 bacterium, the third group was inoculated with the irrelevant control mutant B5, and the fourth group was inoculated with the hemolysinA mutant C93. The bladders and kidneys were harvested on day 2, since according to our calibration experiments at this day the highest number of bacteria were present in the bladder, along with the highest number of NK cells. As can be seen in Figure 7F, the groups of mice that did not undergo prior treatments and that were injected with UPEC CFT073 or with the irrelevant mutant (B5) had significantly more bacteria as compared to the C93-injected group. Importantly, in all of the NK cell-depleted groups (the NK cell depletion was verified in the blood of each of the NK1.1-treated mice, prior to the removal of the bladders) and in all of the Etanercept (TNF-α blocker)-treated groups the bacterial load was similar to the untreated B5 and UPEC CFT073 groups (Figure 7F). This indicates that NK cells and TNF-α play a significant role in attenuating/controlling bacterial infection in the bladder in vivo. The UPEC CFT073 bacterium or the mutant C93 bacterium could hardly be detected in the kidneys, irrespective of whether or not NK cells were depleted or whether TNF-α was blocked (Figure 7G). To demonstrate directly that NK cells are responsible for the TNF-α secretion following bacterial inoculation, we took the bladder extracts used to determine the bacterial loads in Figure 7F and measured the TNF-α concentrations. The untreated bladders injected with the C93 mutant had the lowest CFU (Figure 7F), and accordingly the levels of TNF-α were the highest (Figure 7H). In contrast, in the untreated mice injected with the B5 mutant, bacterial loads were elevated (Figure 7F), while the TNF-α levels were reduced by 50% (Figure 7H). When NK cells were depleted, the TNF-α levels were equivalent to those

observed following B5 inoculation, indicating that in response to UPEC CFT073 infection, in the absence of hemolysinA, NK cells secrete TNF-α in vivo.

During acute cystitis, UPEC invade the bladder epithelial cells in a regulated process, named "developmental cycle" (Jorgensen and Seed, 2012), that includes bacterial adhesion, invasion, the formation of intracellular bacterial communities (IBCs) and the release from the tissue via exfoliation. Because NK cells are observed in significant numbers in the bladders only 1 day following the infection (Figure 6B), we assumed that NK cells are not involved in the initial UPEC adhesion and invasion to the uroepithelial cells. We therefore investigated, using TEM, whether IBC can be observed in bladders infected with the C93 mutant bacterium (as the growth of this bacterium is NK cell sensitive; Figure 7F). The experiments were performed on day 2, at the peak of NK cell accumulation. As can be seen in Figure 7I, IBCs were observed in the infected bladders even following C93 inoculation, demonstrating that NK cells probably do not inhibit IBC formation.

DISCUSSION

We started this research by noticing that UPEC CFT073 adheres to NK cells and that binding of this bacterium led to killing of the NK cells. The killing was not dependent on the type of urinary tract infection, i.e., cystitis or pyelonephritis, but rather it occurred when the bacteria expressed the hemolysinA protein. The importance of these findings is highlighted by the fact that UPEC strains are the most common etiological agents responsible for uncomplicated UTI among otherwise healthy women (Ulett et al., 2013). Mutant screening performed at 4°C identified nine mutants defective in adhesion to NK cells. Interestingly, eight of the nine adhesion mutants were defective either in the type I fimbriae genes or in type I fimbriae-related genes. Type I fimbriae produced by more than 80% of all UPEC strains is required for bacterial attachment to mannose residues of the glycoprotein receptor uroplakin Ia on the surface of urinary epithelium cells as well as for bacterial invasion and persistence in target cells (Bouckaert et al., 2006).

After screening more than 1,000 bacterial mutants, we did not find mutants which were defective in the other adhesions used by UPEC to adhere to the uroepithelium such as P (Pap), F1C, S, M, and Dr (Stapleton, 2005). Thus, we concluded that these other adhesion molecules are probably not involved in the UPEC CFT073 adhesion to NK cells. Interestingly, none of the adhesion mutants presented a complete absence of attachment. This may be explained either by the presence of another adhesion protein, composed of several redundant subunits, or by a nonreceptor-mediated binding of UPEC CFT073 to NK cells. Nevertheless, the type I fimbriae play a significant role in bacterial adhesion to NK cells, and when a mutant in which the fimbriae was locked in an "on" orientation was used, approximately 90% of the NK cells bound the bacteria, and this led to a very efficient killing of the NK cells.

Three mutants were identified that were completely defective in their NK killing ability, and all three mutants were disrupted in different genes belonging to the hemolysin operon (*hlyA*, *hlyC*, and *hlyD*). Importantly, hemolysinA is associated with human pathogenic strains of *E. coli* causing clinically severe forms of UTI (Gadeberg et al., 1983). Approximately half of UPEC strains that cause upper UTIs (pyelonephritis) and about a third of those that cause lower UTIs (cystitis) express hemolysinA. This is in contrast to only about 10% of fecal isolates that express hemolysinA. The hemolysinA protein is unique among *E. coli* toxins because it is secreted across both membranes (Cavalieri et al., 1984). The ability of the hemolysin toxin to be secreted via outer-membrane vesicles (Balsalobre et al., 2006) may explain why the adhesion mutants were still able to efficiently kill NK cells and may also explain why dead NK cells are seen in the presence of UPEC CFT073, even when the

bacteria are not directly attached to them. Still, as mentioned above, for efficient killing of NK cells bacterial adhesion to NK cells is required.

NK cells were particularly sensitive to the hemolysin-mediated killing, whereas human T cells were almost completely resistant. The reason for this hemolysinA-mediated hypersensitivity of NK cells is unknown. Virtually nothing is known about the sensitivity of lymphocytes to hemolysinA-mediated killing. A literary search identified one paper, from 1983 (Gadeberg et al., 1983), which presents data which supports our findings. The authors showed that hemolysinA was toxic to monocytes and granulocytes, and lymphocytes were relatively resistant, whereas NK cells, which had been discovered less than a decade beforehand, were not tested (Gadeberg et al., 1983). Indeed, we also observed that neutrophils were efficiently killed by the hemolysinA-expressing bacteria (data not shown).

It was previously shown that hemolysinA can trigger rapid degradation of paxillin as well as other host proteins and that it also causes serine proteases and caspase activation which promote apoptosis of the host cells (Dhakal and Mulvey, 2012). This explains why, in addition to lysing erythrocytes and killing of NK cells (shown here), hemolysinA is toxic to a range of host cells. Interestingly, it was also shown (Dhakal and Mulvey, 2012; König et al., 1994) that in addition to tissue injury, hemolysinA can indirectly disrupt various aspects of host cell signaling and suppress cytokine (such as IL-6 and TNF-α) release from human lymphocytes/monocytes and basophils. Thus, hemolysinA impairs TNF-α activity in numerous ways: by killing NK cells directly, as shown here, and indirectly, by impairing host cell signaling as shown previously.

To evaluate the role played by NK cells in UTI, we initially established that NK cells are absent from the bladder when no infection is present and that they accumulate in the bladder upon UTI induction. Because the NK cell numbers decreased in the blood following the bacterial inoculation, we suggest that NK cells are recruited to the bladder and kidney, at least partially, from the blood.

Mice are not the best model for studying UTI, as they abundantly express TLR-11 in their bladder and kidneys, whereas this TLR is absent in humans (Lauw et al., 2005; Zhang et al., 2004). This leads to TLR-11-dependent bacterial clearance (Zhang et al., 2004). Indeed, we observed that 5–6 days postinfection the mice were free of bacteria, irrespective of whether NK cells were present or absent and independently of the type of injected bacteria. Nevertheless, despite the limitations of this in vivo model, we were able to convincingly demonstrate that NK cells are important for UTI attenuation in vivo. While no direct killing of the bacteria was observed, we demonstrated both in vitro and in vivo that NK cells secrete large amounts of TNF-α in response to nonhemolytic UPEC infection. When we blocked TLR-4, we observed a partial reduction in TNF-α secretion, suggesting that TLR-4 partially participates in production of TNF-α from NK cells following direct interaction with UPEC and that another receptor(s) whose identity is currently unknown can also sense UPEC and secrete TNF-α. Supporting these observations, it was shown that NK cells secrete TNF-α via TLR-4 in response to stimulation via FimH and LPS of UPEC (Mian et al., 2010). Finally, we also demonstrate that IBCs are still observed in the bladders of mice infected with the NK-sensitive strain C93. It will be interesting to thoroughly study in the future whether and how NK cells affect the UPEC developmental cycle in the uroepithelial cells.

In summary, we discovered a host defense and microbial counterattack mechanism in which NK cells control UTI and UPEC retaliates by killing the NK cells using hemolysinA.

EXPERIMENTAL PROCEDURES

Mice

All experiments were performed using 6- to 8-week-old C57BL/6 female mice. The generation of the *Ncr1*$^{gfp/+}$ mice was described previously (Gazit et al., 2006). All experiments were performed in accordance with the guidelines of the local ethics committee.

Cells, Plasmids, and Bacterial Strains

Primary human and mouse NK cells were isolated from PBLs of various healthy donors and various mice, respectively, using the human and mouse NK cell isolation kits and the autoMACS instrument according the manufacturer instructions (Miltenyi Biotec). Some of the bacterial strains and the plasmids used in this study are described in Figure S1 and in Tables S1A and S1B.

Creation of UPEC CFT073 Transposon Library, Mutant Screen, Bacterial Adhesion, and Killing Assays

EZ::TnKan transposomes (Bahar et al., 2009) were purified from the pMODKan plasmid according to manufacturer's instructions and electroporated into the UPEC CFT073 bacteria harboring the GFP pCM18 plasmid. Primary NK cells (either human or mice) were washed twice with RPMI 1640 without antibiotics and incubated with the various bacteria (mutants or wild-type) at various bacterial to NK cells ratios as indicated. Incubations were performed, for various time points, as indicated, usually, for 3 hr, either at 4°C to determine adhesion or at 37°C to determine NK cell killing, and cells were analyzed by flow cytometry.

Determining the Transposon Location

Genomic DNA was purified from the selected clones (GenElute, Sigma) and restricted with HpaI, MfeI, and NdeI (New England Biolabs) which do not cleave within the inserted transposon. The resulting fragments were then self-ligated (TaKaRa) and used as a template for inverse PCR (Herculase II, Agilent) for amplification of the transposons' flanking sequences. The generated sequences were blasted against the CFT073 genome to determine the location of the insertion mutation.

Hemolysis and Hemolysis Quantification

Bacteria were streaked on blood agar plates supplemented with the appropriate antibiotic, and hemolysis was determined visually by a clear zone around the colony. Colonies were viewed using a Zeiss stemi SVII microscope at an 30.6 magnification and photographed using Infinity I camera. Hemolysis quantification was performed as described previously (Warawa et al., 1999).

In Vivo Assays and Determination of Bacterial Loads

Female mice 6–8 weeks of age were anesthetized with Ketamine and Xylazine before catheter insertion and then infected with 10^8 bacteria in 50 μl of sterile PBS. Tissue samples were homogenized using a Fastprep (MP Biomedicals, USA), serially diluted, and spread on Maconkey plates (Novamed, Israel). Plates were incubated overnight, and colonies were enumerated.

Europe PMC Funders Author Manuscripts

Cytokine Secretion Assays

Various bacteria were incubated with murine NK cells at a ratio of 10:1 for 5 hr at 37°C, 5% CO2. Supernatants were collected, and TNF-α levels were determined using standard ELISA.

NK Cell Depletion and Etanercept Treatment

Mice were injected i.p with 100 μg anti-NK1.1 Ab (PK136) in 200 μl of sterile PBS. The mAb was injected 1 day prior to and 1 day after bacterial inoculation. Sterile PBS was injected as a control. Depletion was verified in all treated mice, prior to bladder removal. To block TNF-α, a soluble receptor (Etanercept) was injected. Each mouse received 0.4 mg of Etanercept once a day, on the day of catheterization, following bacterial inoculation and 1 day later.

Statistical Methods

For statistical significance, Student's t test analysis was used. A statistical test was considered significant (*) when $p < 0.05$. ANOVA was used to identify significant group differences.

Supplementary Material

Refer to Web version on PubMed Central for supplementary material.

Acknowledgments

This study was supported by the Advanced ERC grant, by The Israeli Science Foundation, by The Israeli- I-CORE, by the GIF Foundation, and by The ICRF Professorship Grant (all to O.M.) and by the Israeli Science Foundation (to G.B.). The work was also supported by the Israeli Science Foundation (to C.G.). O.M. is a Crown Professor of Molecular Immunology. C.G. is supported by the Foulkes Foundation. The authors would like to thank Professors Hirotada Mori and Toru Nakayashiki for useful discussion. The authors would also like to thank Professor Saul Burdman, who kindly supplied the pMODkan plasmid. The pGNH404 plasmid was a gift from Professor Agneta Richter-Dahlfors. Bacterial strains CFT073, UPEC76, CFT073ON, CFT073OFF, and CFT fim/pap were from Professor Harry Mobley's collection. The authors thank Professor Ilan Rosenshine for the EPEC E2348/69 strain and Professor Nahum Shpigel for the UTI89 and UTI536 strains. The authors are grateful to the EM Unit of Core Research Facility of the Faculty of Medicine, The Hebrew University Jerusalem, for assistance with electron microscopy.

REFERENCES

Bahar O, Goffer T, Burdman S. Type IV Pili are required for virulence, twitching motility, and biofilm formation of acidovorax avenae subsp. Citrulli. Mol. Plant Microbe Interact. 2009; 22:909–920. [PubMed: 19589067]

Balsalobre C, Silván JM, Berglund S, Mizunoe Y, Uhlin BE, Wai SN. Release of the type I secreted alpha-haemolysin via outer membrane vesicles from Escherichia coli. Mol. Microbiol. 2006; 59:99–112. [PubMed: 16359321]

Bouckaert J, Mackenzie J, de Paz JL, Chipwaza B, Choudhury D, Zavialov A, Mannerstedt K, Anderson J, Piérard D, Wyns L, et al. The affinity of the FimH fimbrial adhesin is receptor-driven and quasi-independent of Escherichia coli pathotypes. Mol. Microbiol. 2006; 61:1556–1568. [PubMed: 16930149]

Cavalieri SJ, Bohach GA, Snyder IS. Escherichia coli alpha-hemolysin: characteristics and probable role in pathogenicity. Microbiol. Rev. 1984; 48:326–343. [PubMed: 6394977]

Chaushu S, Wilensky A, Gur C, Shapira L, Elboim M, Halftek G, Polak D, Achdout H, Bachrach G, Mandelboim O. Direct recognition of Fusobacterium nucleatum by the NK cell natural cytotoxicity receptor NKp46 aggravates periodontal disease. PLoS Pathog. 2012; 8:e1002601. [PubMed: 22457623]

Dhakal BK, Mulvey MA. The UPEC pore-forming toxin α-hemolysin triggers proteolysis of host proteins to disrupt cell adhesion, inflammatory, and survival pathways. Cell Host Microbe. 2012; 11:58–69. [PubMed: 22264513]

Emody L, Kerényi M, Nagy G. Virulence factors of uropathogenic Escherichia coli. Int. J. Antimicrob. Agents. 2003; 22(Suppl 2):29–33. [PubMed: 14527768]

Engel D, Dobrindt U, Tittel A, Peters P, Maurer J, Gütgemann I, Kaissling B, Kuziel W, Jung S, Kurts C. Tumor necrosis factor alpha- and inducible nitric oxide synthase-producing dendritic cells are rapidly recruited to the bladder in urinary tract infection but are dispensable for bacterial clearance. Infect. Immun. 2006; 74:6100–6107. [PubMed: 16966414]

Gadeberg OV, Orskov I, Rhodes JM. Cytotoxic effect of an alpha-hemolytic Escherichia coli strain on human blood monocytes and granulocytes in vitro. Infect. Immun. 1983; 41:358–364. [PubMed: 6345395]

Gazit R, Gruda R, Elboim M, Arnon TI, Katz G, Achdout H, Hanna J, Qimron U, Landau G, Greenbaum E, et al. Lethal influenza infection in the absence of the natural killer cell receptor gene Ncr1. Nat. Immunol. 2006; 7:517–523. [PubMed: 16565719]

Halfteck GG, Elboim M, Gur C, Achdout H, Ghadially H, Mandelboim O. Enhanced in vivo growth of lymphoma tumors in the absence of the NK-activating receptor NKp46/NCR1. J. Immunol. 2009; 182:2221–2230. [PubMed: 19201876]

Hannan TJ, Mysorekar IU, Chen SL, Walker JN, Jones JM, Pinkner JS, Hultgren SJ, Seed PC. LeuX tRNA-dependent and -independent mechanisms of Escherichia coli pathogenesis in acute cystitis. Mol. Microbiol. 2008; 67:116–128. [PubMed: 18036139]

Haraoka M, Hang L, Frendéus B, Godaly G, Burdick M, Strieter R, Svanborg C. Neutrophil recruitment and resistance to urinary tract infection. J. Infect. Dis. 1999; 180:1220–1229. [PubMed: 10479151]

Jewett A, Gan XH, Lebow LT, Bonavida B. Differential secretion of TNF-alpha and IFN-gamma by human peripheral blood-derived NK subsets and association with functional maturation. J. Clin. Immunol. 1996; 16:46–54. [PubMed: 8926285]

Johnson JR. Virulence factors in Escherichia coli urinary tract infection. Clin. Microbiol. Rev. 1991; 4:80–128. [PubMed: 1672263]

Jones-Carson J, Balish E, Uehling DT. Susceptibility of immunodeficient gene-knockout mice to urinary tract infection. J. Urol. 1999; 161:338–341. [PubMed: 10037434]

Jorgensen I, Seed PC. How to make it in the urinary tract: a tutorial by Escherichia coli. PLoS Pathog. 2012; 8:e1002907. [PubMed: 23055921]

Kaper JB, Nataro JP, Mobley HL. Pathogenic Escherichia coli. Nat. Rev. Microbiol. 2004; 2:123–140. [PubMed: 15040260]

Koch J, Steinle A, Watzl C, Mandelboim O. Activating natural cytotoxicity receptors of natural killer cells in cancer and infection. Trends Immunol. 2013; 34:182–191. [PubMed: 23414611]

König B, Ludwig A, Goebel W, König W. Pore formation by the Escherichia coli alpha-hemolysin: role for mediator release from human inflammatory cells. Infect. Immun. 1994; 62:4611–4617. [PubMed: 7523294]

Kucheria R, Dasgupta P, Sacks SH, Khan MS, Sheerin NS. Urinary tract infections: new insights into a common problem. Postgrad. Med. J. 2005; 81:83–86. [PubMed: 15701738]

Lauw FN, Caffrey DR, Golenbock DT. Of mice and man: TLR11 (finally) finds profilin. Trends Immunol. 2005; 26:509–511. [PubMed: 16111920]

Mian MF, Lauzon NM, Andrews DW, Lichty BD, Ashkar AA. FimH can directly activate human and murine natural killer cells via TLR4. Mol. Ther. 2010; 18:1379–1388. [PubMed: 20442710]

Mobley HL, Jarvis KG, Elwood JP, Whittle DI, Lockatell CV, Russell RG, Johnson DE, Donnenberg MS, Warren JW. Isogenic P-fimbrial deletion mutants of pyelonephritogenic Escherichia coli: the role of alpha Gal(1-4) beta Gal binding in virulence of a wild-type strain. Mol. Microbiol. 1993; 10:143–155. [PubMed: 7968511]

Ragnarsdóttir B, Lutay N, Grönberg-Hernandez J, Köves B, Svanborg C. Genetics of innate immunity and UTI susceptibility. Nat. Rev. Urol. 2011; 8:449–468. [PubMed: 21750501]

Seidel E, Glasner A, Mandelboim O. Virus-mediated inhibition of natural cytotoxicity receptor recognition. Cell. Mol. Life Sci. 2012; 69:3911–3920. [PubMed: 22547090]

Sivick KE, Schaller MA, Smith SN, Mobley HL. The innate immune response to uropathogenic Escherichia coli involves IL-17A in a murine model of urinary tract infection. J. Immunol. 2010; 184:2065–2075. [PubMed: 20083670]

Stapleton A. Novel mechanism of P-fimbriated Escherichia coli virulence in pyelonephritis. J. Am. Soc. Nephrol. 2005; 16:3458–3460. [PubMed: 16280466]

Totsika M, Heras B, Wurpel DJ, Schembri MA. Characterization of two homologous disulfide bond systems involved in virulence factor biogenesis in uropathogenic Escherichia coli CFT073. J. Bacteriol. 2009; 191:3901–3908. [PubMed: 19376849]

Ulett GC, Totsika M, Schaale K, Carey AJ, Sweet MJ, Schembri MA. Uropathogenic Escherichia coli virulence and innate immune responses during urinary tract infection. Curr. Opin. Microbiol. 2013; 16:100–107. [PubMed: 23403118]

Warawa J, Finlay BB, Kenny B. Type III secretion-dependent hemolytic activity of enteropathogenic Escherichia coli. Infect. Immun. 1999; 67:5538–5540. [PubMed: 10496946]

Wiles TJ, Kulesus RR, Mulvey MA. Origins and virulence mechanisms of uropathogenic Escherichia coli. Exp. Mol. Pathol. 2008; 85:11–19. [PubMed: 18482721]

Zhang D, Zhang G, Hayden MS, Greenblatt MB, Bussey C, Flavell RA, Ghosh S. A toll-like receptor that prevents infection by uropathogenic bacteria. Science. 2004; 303:1522–1526. [PubMed: 15001781]

Europe PMC Funders Author Manuscripts

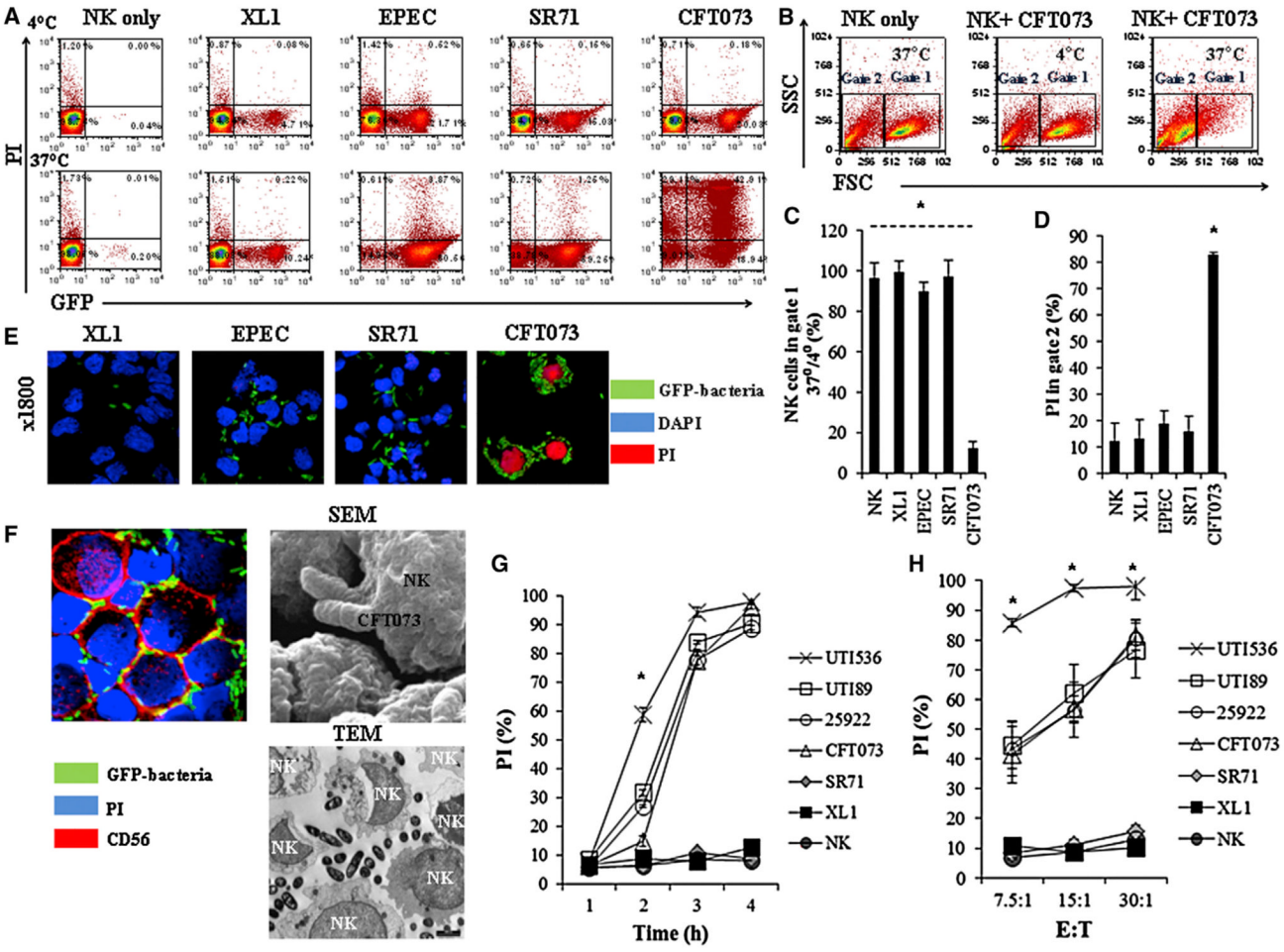

Figure 1. UPEC Kill Human NK Cells

(A) Flow cytometry analysis of various GFP-expressing strains of *E. coli* (indicated above the quadrants) incubated with primary human NK cells and stained with PI (y axis). The bacterium to NK ratio was 30:1, and incubations were performed for 3 hr either at 4°C (upper quadrants) or at 37°C (lower quadrants). The percentages of NK cells in each quadrant are indicated.

(B) Forward and side scatter analysis of NK cells incubated with or without UPEC CFT073, at 4°C or at 37°C (indicated inside the quadrants). Gate 1 shows live human NK cells, and gate 2 shows the nonviable ones.

(C) Ratios ×100 of viable NK cells present in gate 1 following 3 hr of incubation with the indicated bacteria at 37°C were divided by the number of NK cells incubated with the same bacteria for 3 hr at 4°C.

(D) Percentages of PI-positive NK cells present in gate 2 following 3 hr incubation at 37°C with the various GFP expression *E. coli* strains, indicated in the x axis.

(E) Confocal microscopy of PI-stained human NK cells incubated with different GFP expressing *E. coli* strains for 3 hr at 37°C. The different bacteria are indicated by green staining, DAPI is in blue, and PI is in red. Magnification ×1,800.

(F) Confocal microscopy, SEM, and TEM of human NK cells incubated with UPEC CFT073 for 3 hr at 37°C. The bacterium to NK cells ratio was 30:1. The bacteria seen in the

Europe PMC Funders Author Manuscripts

confocal microscopy are indicated by green staining, PI is in blue, and the anti-CD56 staining is in red. The TEM and SEM pictures are marked.

(G) Shown are percentages of PI-positive NK cells following incubation of NK cells at 37°C with the indicated bacteria at various time points (indicated in the x axis). The bacterium to NK cells ratio was 30:1.

(H) Percentages of PI-positive NK cells following 3 hr incubation at 37°C with the indicated *E. coli* strains at several bacteria to NK cells ratios (indicated at the x axis). Figures show one representative experiment out of at least three independent experiments performed and an average ±SD of duplicate in (C), (D), (G), and (H). For (C) and (D), *$p < 0.00001$ for UPEC CFT073 versus all other bacteria. For (G) and (H) *$p < 0.01$ for UTI536 versus all other bacteria. 25922 represent ATCC 25922. See also Table S1 and Figure S1.

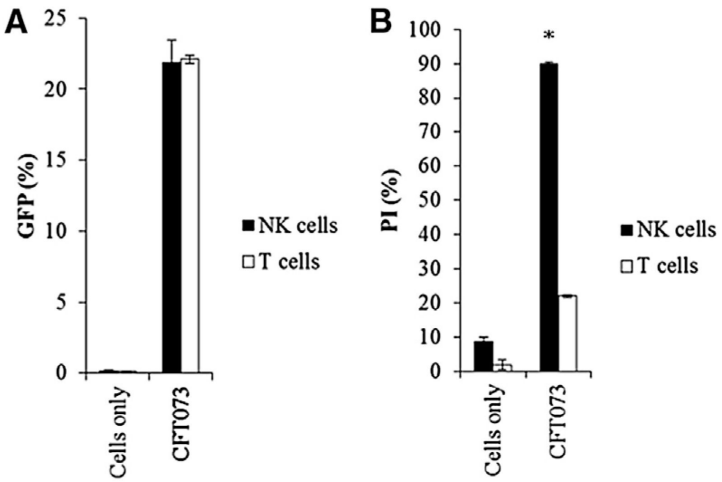

Figure 2. UPEC CFT073 Preferentially Kills NK Cells

(A) Adhesion of UPEC CFT073 to human NK and T cells was determined by percentages of GFP-positive cells following 3 hr incubation at 4°C.

(B) Killing of human NK and T cells following 3 hr incubation at 37°C with UPEC CFT073 was determined by the percentages of cells stained with PI. Figures show a representative of three independent experiments, and an average ±SD of duplicate is presented. *$p < 0.0005$.

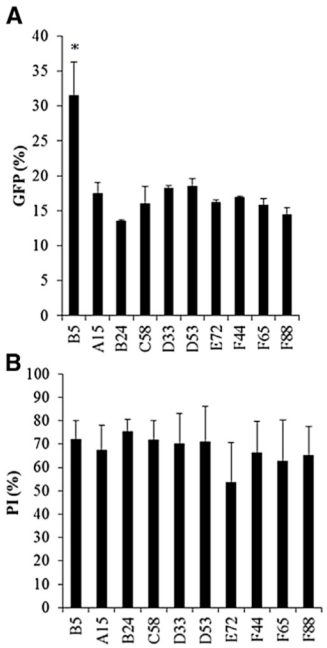

E

Mutant #	Disrupted gene	Putative disruptive function
A15	*fimB*	Regulator of *fimA* operon
B24	*truA*	tRNA uridine
C58	*fimC*	Fim proteins translocation
D33	*fimB*	Regulator of *fimA* operon
D53	*dsbB*	Disulfide bond formation
E72	*C3637*	Sialic acid transporter
F44	*dam*	DNA adenine methylase
F65	*dsbA*	Disulfide bond formation
F88	*fimI*	Unknown
C93	*hlyA*	Hemolysin toxin
E49	*hlyC*	Hemolysin acylation
D57	*hlyD*	Hemolysin secretion
B5	Hypothetical gene	Unknown

Figure 3. Transposon-Based Mutagenesis Identifies Type I Fimbriae and HemolysinA

(A) More than 1,000 GFP-expressing UPEC CFT073 mutants were screened for adhesion to primary human NK cells at 4°C (A and C, determined by percentages of GFP-positive NK cells) and for killing of human NK cells at 37°C (B and D determined by PI-positive NK cells). B5, an irrelevant mutant of UPEC CFT073 was used as a control. Data are representative of at least three independent analyses of the relevant mutants. Data are represented as mean ± SEM. *$p < 0.001$. (E) Table summarizing the transposon location in the disrupted genes of relevant mutants. The adhesion mutants are in white, the hemolysinA mutants are in dark gray, and the irrelevant mutant B5 (bottom) is in light gray. See also Figure S2.

Europe PMC Funders Author Manuscripts

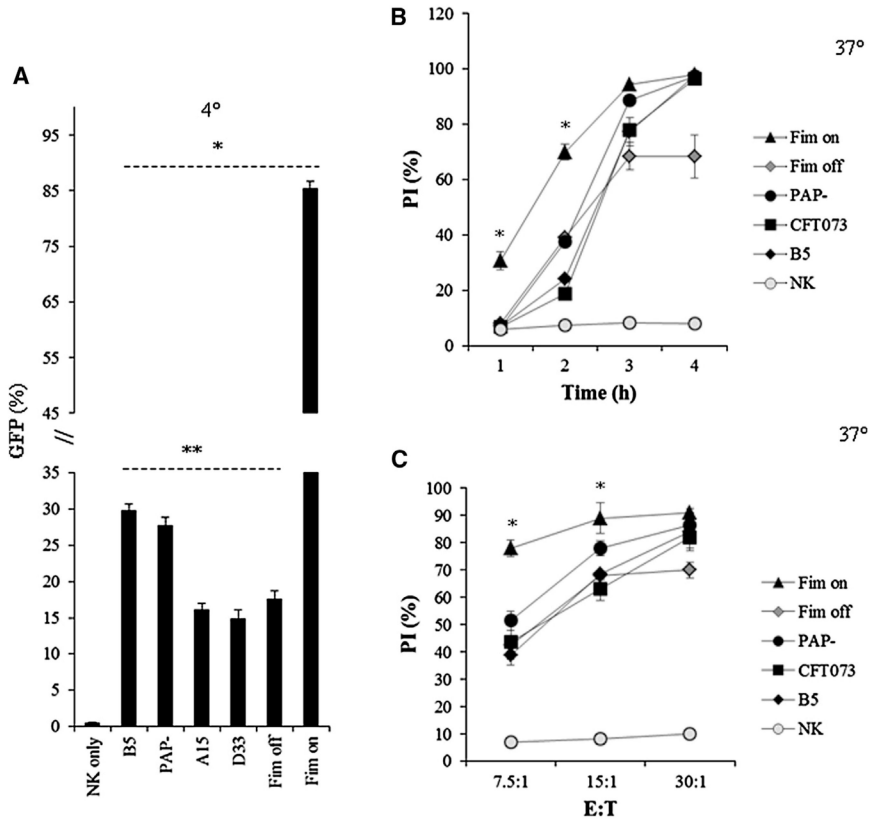

Figure 4. Increased Type I Fimbriae-Mediated Attachment Leads to an Increase in Killing of Human NK Cells

(A) Percentages of binding of human NK cells following 3 hr of incubation with GFP-expressing bacteria indicated in the x axis. Binding was performed at 4°C and was calculated by the percentages of GFP-positive NK cells. *$p < 0.0001$ for Fim on versus all other bacteria, **$p < 0.01$ for B5 and PAP– versus A15, D33, and Fim off.

(B and C) Killing of human NK cells at 37°C following incubation with the GFP-labeled bacteria, indicated in the legend, at several time points (B) and at various bacteria to NK cells (E:T) ratios (C). The percentages of NK cell killing by the various bacteria were determined by PI staining. Data are a representative of three independent experiments and an average ± SD of duplicate is shown. For (B) and (C), *$p < 0.001$ for Fim on bacteria versus all other bacteria.

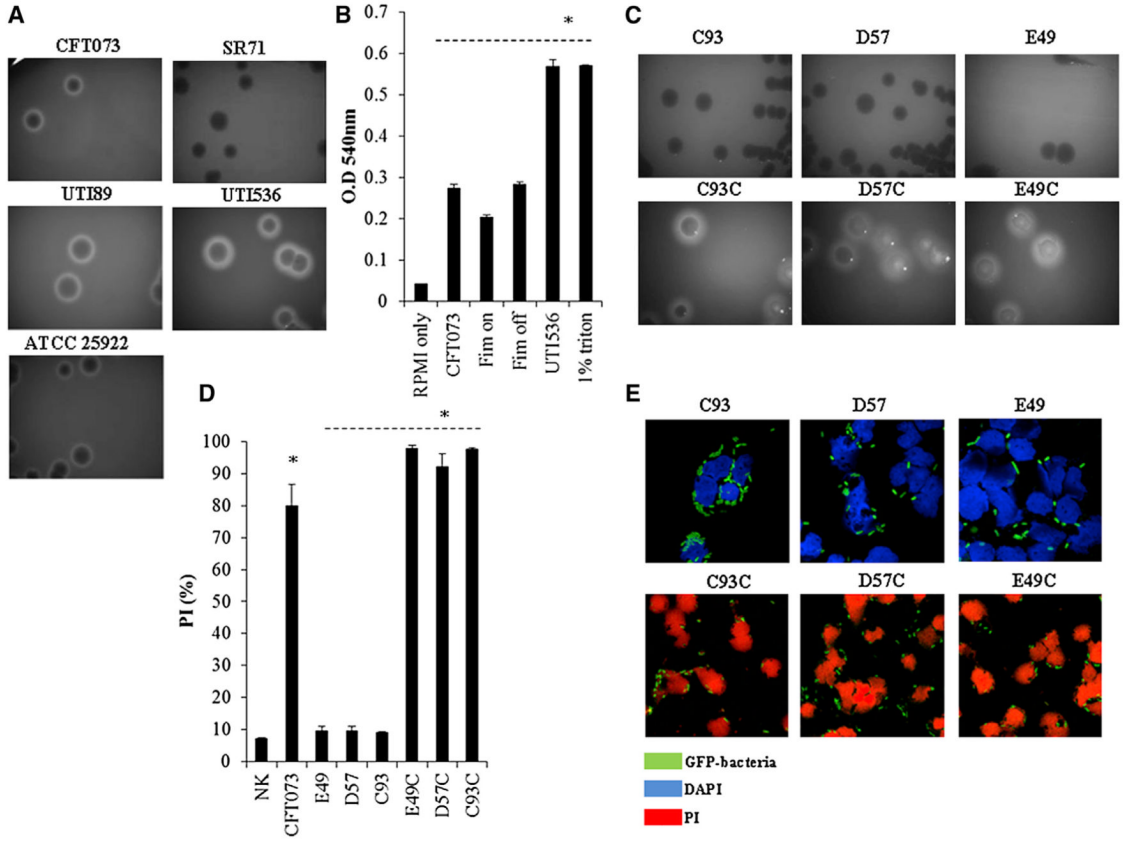

Figure 5. Hemolytic Bacteria Kill NK Cells

(A) Hemolysis of sheep RBCs was mediated by CFT073, ATCC 25922, UTI89, UTI536, and SR71 UPEC strains streaked on blood agar plates.

(B) Quantification of sheep RBCs hemolysis (represented in the y axis by O.D) induced by UPEC CFT073, the Fim on and Fim off mutants, and the UPEC UTI536 strains. RBCs treated with 1% triton were used as a positive control, and treatment with RPMI (phenol red minus) was used as a negative control. *$p < 0.01$ for UTI536 and 1% triton versus all other bacteria.

(C) Hemolysis was mediated by the hemolysinA mutants (C93, D57, and E49, upper panels) and by the complemented hemolysinA bacteria (C93C, D57C, and E49C, lower panels).

(D and E) Killing of NK cells by wild-type UPEC CFT073 bacterium, by the hemolysinA mutants (C93, D57, and E49) and by the complemented bacteria (C93C, D57C, and E49C) at 37°C, determined either by flow cytometry (D) or by using confocal microscopy (E). One of three (A, C, and E) or four (B and D) independent experiments is shown. An average ±SD of duplicate is shown in (B) and (D). In (D), *$p < 0.0001$ for UPEC CFT073 and E49C, D57C, and C93C versus E49, D57, and C93. See also Figure S3.

Europe PMC Funders Author Manuscripts

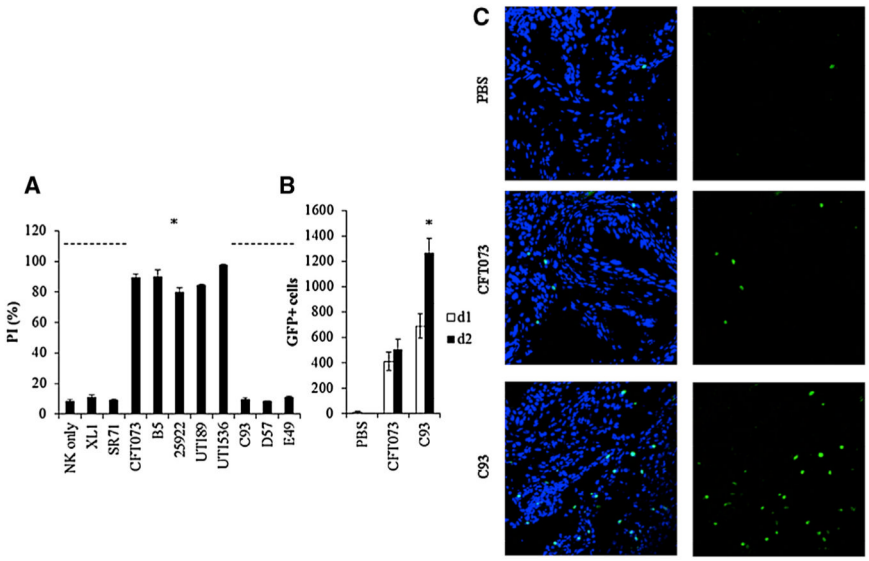

Figure 6. NK Cells Accumulate in the Bladder following UPEC CFT073 Infection

(A) Percentages of PI-positive murine NK cells incubated at 37°C for 3 hr with wild-type hemolytic (CFT073, ATCC 25922, UTI89, UTI536) and nonhemolytic (XL1, SR71) UPEC bacteria, with the irrelevant mutant B5 or with the hemolysinA-deficient mutants (C93, D57, and E49). *$p < 0.005$ for CFT073, B5, ATCC 25922, UTI89, and UTI536 versus all other bacteria.

(B) Number of GFP-positive NK cells in the bladder on day 1 and on day 2 following infection with UPEC CFT073 or with the hemolysinA-deficient C93 mutant. Injection of PBS was used as control (five to eight mice were used in each group). *$p < 0.005$ for NK cells present in the bladders injected with C93 on day 2 versus day 1 and versus day 2-injected UPEC CFT073 bladders.

(C) Representative confocal microscopy images of uroepithelial cells obtained from murine bladders injected with PBS (top), with wild-type UPEC CFT073 (middle), or with the hemolysinA-deficient mutant C93 (bottom). NK cells are visualized by GFP. Left panels depict merge staining of DAPI-stained bladder cells with the GFP-labeled NK cells; right panels show the NK cells only. For (A) and (B), data are a representative of three independent experiments, and an average ±SD of triplicate is shown. Slides for confocal microscopy were prepared from four to eight bladders of mice in each group and were taken from two independent experiments on day 2 of UTI induction. 25922 stands for ATCC 25922. See also Figure S4.

Europe PMC Funders Author Manuscripts

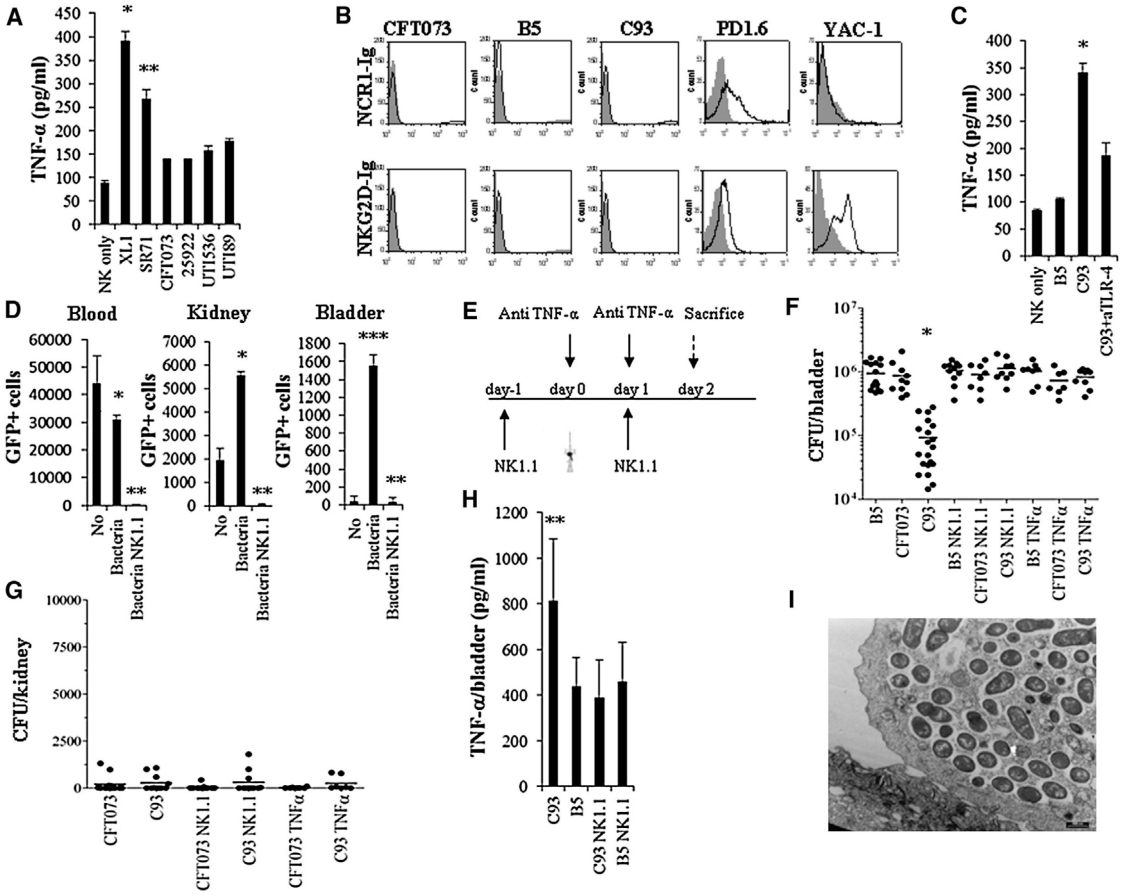

Figure 7. NK Cells Secrete TNF-α to Protect against UTI

(A) ELISA assays for TNF-α secretion (concentration represented as picogram/ml, pg/ml) from NK cells following 5 hr of incubation with the hemolytic (CFT073, ATCC 25922, UTI89, UTI536) and nonhemolytic (XL1, SR71) UPEC bacteria at 37°C. *$p < 0.005$ for XL1 versus all other hemolytic bacteria. Data are represented as mean ± SEM. **$p < 0.01$ for SR71 versus all other hemolytic bacteria.

(B) FACS staining of UPEC CFT073, the hemolysinA-deficient mutant C93, the irrelevant mutant B5, PD1.6 and YAC-1 cells with NCR1-Ig, and with the NKG2D-Ig fusion proteins (staining is indicated by the black empty histograms). The gray-filled histogram represents staining with control Ig-fusion protein.

(C) ELISA assays for TNF-α secretion from murine NK cells following 5 hr of incubation with the irrelevant mutant B5 and the hemolysinA-deficient mutant C93. NK cells incubated with the C93 bacterium were coincubated with or without blocking anti-TLR-4 mAb. Data are represented as mean ± SEM. *$p < 0.01$ for C93 in the absence of anti-TLR-4 mAb versus C93 in the presence of anti-TLR-4 mAb.

(D) Numbers of GFP-positive NK cells in the blood, kidneys, and bladders of mice treated with sterile PBS only or injected with the hemolysinA-deficient mutant C93 with or without NK cell depletion using anti-NK1.1 mAb. *$p < 0.01$ for mice injected with the bacteria versus no bacteria. Data are represented as mean ± SEM. **$p < 0.0001$ for NK1.1-treated mice versus all other mice. ***$p < 0.001$ for bacteria in the bladders following UTI versus no bacteria or versus NK cell depletion.

Europe PMC Funders Author Manuscripts

(E) Schematic representation of the in vivo experiment. The catheter in the figure indicates the day of UTI induction.
(F and G) Bacterial loads in the bladders (F) and kidneys (G) as determined by colony-forming units (CFU) on day 2 following bacterial injection. Mice were treated with anti-NK1.1 (NK1.1), with Etanercept (TNF-α), or with PBS as described in (E) and infected with UPEC CFT073, the mutant B5, or the hemolysinA-deficient C93 mutant. Data are represented as mean ± SEM. *$p < 0.05$ for mice inoculated with C93 only versus all other injections.
(H) ELISA assays for the presence of TNF-α in the infected bladders derived from (F). Three to five bladders were obtained from each group. Data are represented as mean ± SEM. **$p < 0.01$ for C93-injected treated mice versus all other mice.
(I) TEM was performed 2 days following C93 injections into the bladder. Data in (A)–(D) and (I) is a representative of two independent experiments. The data presented in (F)–(H) is a summary of two independent experiments. See also Figure S5.

Europe PMC Funders Author Manuscripts